Received Date: 24-Mar-2016 Revised Date : 21-Oct-2016 Accepted Date: 25-Oct-2016

Article type : Primary Research Articles

**Title:** Response of Sierra Nevada forests to projected climate-wildfire interactions

Running head: Forest response to projected climate-wildfire

**Authors:** Shuang Liang<sup>1</sup>, Matthew D. Hurteau<sup>2</sup>\*, A. LeRoy Westerling<sup>3</sup>

### Affiliation:

<sup>1</sup>Intercollege Graduate Degree Program in Ecology and Department of Ecosystem Science and Management, The Pennsylvania State University, 228 Forest Resources Building, University Park, PA 16802 (sul248@psu.edu)

<sup>2</sup>Department of Biology, University of New Mexico, MSC03 2020, Albuquerque, NM 87131 <sup>3</sup>Sierra Nevada Research Institute, University of California, Merced, 5200 N. Lake Road, Merced, CA 95343 (awesterling@ucmerced.edu)

\*Corresponding Author:

Matthew D. Hurteau Tel: 505-277-0863 Fax: 505-277-0304

E-mail: mhurteau@unm.edu

**Keywords:** climate change, wildfire, carbon, forest community change, LANDIS-II, Sierra

Nevada

**Type of Paper:** Primary Research Article

### **Abstract**

Climate influences forests directly and indirectly through disturbance. The interaction of climate change and increasing area burned has the potential to alter forest composition and community assembly. However, the overall forest response is likely to be influenced by species-specific responses to environmental change and the scale of change in overstory species cover. In this study, we sought to quantify how projected changes in climate and large wildfire size would alter forest communities and carbon (C) dynamics, irrespective of competition from non-tree species and potential changes in other fire regimes, across the Sierra Nevada, USA. We used a species-specific, spatially explicit forest landscape model (LANDIS-II) to evaluate forest response to climate-wildfire interactions under historical (baseline) climate and climate projections from three climate models (GFDL, CCSM3 and CNRM) forced by a medium-high emission scenario (A2) in combination with corresponding climate-specific large wildfire projections. By late-century, we found modest changes in the spatial distribution of dominant species by biomass relative to baseline, but extensive changes in recruitment distribution. Although forest recruitment declined across much of the Sierra, we found that projected climate and wildfire favored the recruitment of more drought-tolerant

This article has been accepted for publication and undergone full peer review but has not been through the copyediting, typesetting, pagination and proofreading process, which may lead to differences between this version and the Version of Record. Please cite this article as

doi: 10.1111/gcb.13544

This article is protected by copyright. All rights reserved.

species over less drought-tolerant species relative to baseline, and this change was greatest at mid-elevations. We also found that projected climate and wildfire decreased tree species richness across a large proportion of the study area and transitioned more area to a C source, which reduced landscape-level C sequestration potential. Our study, although a conservative estimate, suggests that by late-century forest community distributions may not change as intact units as predicted by biome-based modeling, but are likely to trend toward simplified community composition as communities gradually disaggregate and the least tolerant species are no longer able to establish. The potential exists for substantial community composition change and forest simplification beyond this century.

### Introduction

Climate influences forests directly through its differential effects on tree species and indirectly through disturbance. Climate-induced drought stress (Williams *et al.*, 2012) and climate-enhanced large wildfire activity (Westerling *et al.*, 2006; Westerling, 2016) are anticipated to cause changes in forest community composition and productivity, which are likely to affect carbon (C) dynamics (Williams *et al.*, 2007; Lenihan *et al.*, 2008; Loudermilk *et al.*, 2013; Gonzalez *et al.*, 2015). However, there is often a disparity between changes in forest community composition at the landscape scale and the magnitude of environmental change (Jones *et al.*, 2009; Bertrand *et al.*, 2011; Zhu *et al.*, 2012; Svenning & Sandel, 2015). While environmental change can shift the fundamental niche space for successful reproduction of some species, change of overstory species composition is much slower because mature trees are typically more tolerant of a broader range of abiotic conditions (Dolanc *et al.*, 2013; Svenning & Sandel, 2015). Understanding how the interaction of changing climate and climate-driven changes in disturbance regime will influence tree species distributions is central to understanding how these factors will alter forest communities across large landscapes.

Climate has long been identified as a primary control on species occurrence, with speciesspecific environmental tolerance largely determining where species occur along a climate gradient (Woodward et al., 2004; McKenney et al., 2007). Temperature and precipitation are the climate variables that most directly affect vegetation biogeography. Changes in these variables are anticipated to influence species distributions and thus community assemblage (Woodward et al., 2004; Williams et al., 2007; Lutz et al., 2010). With the exception of extreme events, such as 'hotter drought' (Williams et al., 2012; Allen et al., 2015), which can cause sudden forest dieback, climatically driven changes in community composition are often gradual and show disequilibrium with climate (Eriksson et al., 1996; Bertrand et al., 2011; Svenning & Sandel, 2015). Change in forest species cover may be delayed relative to the rate of climate change because long-lived tree species can persist on site even if conditions have become unfavorable for recruitment (Svenning & Sandel, 2015). Moreover, in more topographically diverse environments, montane forest species can move relatively shortdistances and remain in the same climate space (Loarie et al., 2009; Scherrer & Körner, 2011). In contrast to the time lag between changing environmental conditions and change of the overstory species assemblage, regeneration is more responsive to climate change with recruitment success affecting species distribution and forest community assemblage in the long run (Grubb, 1972; Mok et al., 2012; Zhu et al., 2012).

Climate can also indirectly modify forested landscapes through its effects on wildfire regimes (Westerling *et al.*, 2011a; Littell *et al.*, 2009). Interannual and decadal climatic variability has been found to cause regional synchrony in large fire years and area burned in the western US (Heyerdahl *et al.*, 2008a; Westerling, 2016). The relationship between climate variation and

wildfire activity varies regionally and includes factors such as timing of snowmelt (fire season length), vegetation growth (fuel availability), and biomass moisture (fuel flammability) (Heyerdahl *et al.*, 2008b; Gill & Taylor, 2009; Trouet *et al.*, 2010; Taylor & Scholl, 2012). Increasing temperatures and earlier spring snowmelt have been linked to an increase in the frequency of large wildfires in the western US and more frequent large wildfires are projected with continued warming (Westerling *et al.*, 2006, 2011a,b). As area burned increases, the area burned by severe fire is likely to increase (Dillon *et al.*, 2011; Miller & Safford, 2012; Harris & Taylor, 2015), especially when fires burn in dry conditions under extreme fire weather in forests that have homogenized structure resulting from past management actions (McKelvey *et al.*, 1996; Miller *et al.*, 2009; Van Mantgem *et al.*, 2013; Collins, 2014).

The interaction of warmer, drier climate and increasing area burned, coupled with increasing fire severity (e.g., proportion of trees killed) resulting from fire-exclusion (Miller *et al.*, 2009) and past logging activity (McKelvey *et al.*, 1996) has the potential to alter forest composition and community assembly. Species with a higher tolerance to drought and fire may eventually gain competitive advantage over less-tolerant species within the community (Stevens *et al.*, 2015). However, the effects of projected climate-wildfire interactions on forest cover and species distributions may vary as a function of scale. The substantial change of vegetation types projected by biome-based simulation approaches (Bachelet *et al.*, 2001; Hayhoe *et al.*, 2004; Lenihan *et al.*, 2008; Gonzalez *et al.*, 2010) may overestimate the potential for change. The variability in species-specific tolerance to environmental change may drive community composition change, without a concomitant shift in the vegetation type (Zhu *et al.*, 2012; Svenning & Sandel, 2013).

Given the climatic constraints on species recruitment and the dispersal limitations resulting from the increasing extent of high-severity fires (Miller & Safford, 2012), delayed forest recovery could impact forest C dynamics. Fire-induced tree mortality can transition a forest from a C sink to a C source, lowering landscape-level C sequestration potential (Dore *et al.*, 2008). The time required for the burned forest to return to a C sink depends on post-fire succession. If the successional pathway results in re-establishment of the pre-fire community, forest growth will re-sequester the C lost from fire. However, if changes in climate and fire regime slow or alter post-fire succession, the burned area may transition to a lower C state community type and this transition from forest to shrubland or grassland can be reinforced by subsequent burning (Hurteau & Brooks, 2011; Collins & Roller, 2013; Stephens *et al.*, 2013; Lauvaux *et al.*, 2016).

The Sierra Nevada Mountains are occupied by a diversity of tree species and forest types, with distributions being shaped by climate and wildfire patterns that tend to sort by elevation (van Wagtendonk & Fites-Kaufman, 2006). Forest types range from low-elevation dry forests and woodlands to mid-elevation mixed-conifer forests and high-elevation upper montane and subalpine forests. Mid-elevation forest composition has been most impacted by fire-exclusion, transitioning these forests from being dominated by drought-tolerant, fire-resistant pines to drought-intolerant, fire-sensitive firs (McKelvey *et al.*, 1996; Scholl and Taylor, 2010). Given the substantial latitudinal and elevational range that Sierra Nevada forests span and the range of species-specific physiological tolerance to stressors, we asked the question: how will forest composition and community assembly as well as associated C dynamics change across the landscape under projected climate-wildfire interactions? We used a species-specific, spatially explicit landscape modeling approach to evaluate the effects of climate change and climate-driven changes in area burned on forest dynamics. We used

climate projections from three climate models driven by a medium-high emission scenario in combination with corresponding climate-specific large wildfire projections to evaluate the effects of different climate-wildfire scenarios. We hypothesized that: 1) the change in overstory species composition would be less extensive than the change in recruitment because young individuals tolerate a more constrained range of abiotic conditions than mature individuals, 2) projected climate and wildfire would favor the recruitment of drought-tolerant species over drought-intolerant species and that this change would be greatest at midelevations where drought-intolerant species comprise a majority of the forest community, 3) projected climate and wildfire would result in communities with lower species richness, and 4) warmer, drier conditions and larger wildfires would transition more of the landscape to a C source.

Materials and methods Study area description

Our study area comprised approximately  $3.4 \times 10^6$  ha of forested land over the Sierra Nevada Mountains of California and Nevada, USA (Fig.1). Other vegetation types, such as shrubland and grassland, are also distributed across the Sierra Nevada but these vegetation types were not included in our simulations because of computational limitations. Our study area spans a substantial elevation gradient (Fig. S1a). The gradual western slope constitutes the majority of our study area, while the steep eastern slope occupies a narrow strip of the study area (Fig.1). The climate is primarily Mediterranean with dry summers and wet winters (van Wagtendonk & Fites-Kaufman, 2006). More than half of the total precipitation falls as snow, with snowmelt from persistent snowpack providing a source of moisture into summer. Total precipitation varies over the region, decreasing from north to south and from high to low elevation. Precipitation is also higher on the western slope than on the eastern slope, due to the rain shadow effect. Fire activity mainly occurs during the annual drought period when there is little rain (Westerling *et al.*, 2003; Syphard *et al.*, 2011). Soils in the study area are primarily classified as shallow, well-drained Entisols and Inceptisols, but some more developed Alfisonls, Mollisols, and Andisols exist (NRCS, 2013).

Forest type varies by elevation (Fig. S2), with low-elevation forests being more moisture limited and higher-elevation forests being more temperature limited. On the western slope of the study area, the low-elevation forests and woodlands are primarily comprised of gray pine (Pinus sabiniana), ponderosa pine (P. ponderosa) and oaks (Quercus spp.). The midelevation forests are dominated by a mix of conifers including white fir (Abies concolor), Douglas-fir (Pseudotsuga menziesii), ponderosa pine, Jeffrey pine (P. jeffreyi), sugar pine (P. lambertiana) and incense-cedar (Calocedrus decurrens). The upper montane and subalpine forests mainly consist of red fir (A. magnifica), western white pine (P. monticola), mountain hemlock (Tsuga mertensiana), lodgepole pine (P. contorta) and whitebark pine (P. albicaulis). On the eastern slope of Sierra Nevada, the forest communities are similar, but typically occur at higher elevation because of lower precipitation. The primary vegetation differences are a higher proportion of Jeffrey pine at mid-elevation in the eastside forests and the lower elevation eastern woodlands are primarily comprised of singleleaf pinyon pine (P. monophylla). Chaparral communities are persistent at some locations in the Sierra Nevada (Keeley et al., 2005), however, the focus of our study was on tree species and we did not include parameterization for shrub species.

Simulation model framework and parameterization

To project landscape-scale forest dynamics in response to changes in climate and wildfire, we used LANDIS-II, a spatially explicit landscape-scale forest succession and disturbance model using a core-extension framework (Scheller *et al.*, 2007). In the model, species are represented by biomass in age-cohorts and forest succession is based on growth, mortality, and reproduction, as determined by species-specific life history and physiological attributes. To simulate succession and disturbance, we used three extensions for this study: the Century Succession extension (Scheller *et al.*, 2011a, hereafter called 'Century'), the Dynamic Leaf Biomass Fuels extension (Sturtevant *et al.*, 2009; Scheller *et al.*, 2011b, hereafter called 'Dynamic Fuel'), and the Dynamic Fire extension (Sturtevant *et al.*, 2009, hereafter called 'Dynamic Fire').

The core LANDIS-II model requires an initial communities layer that represents the distribution of species age-cohorts across the study area and an ecoregions layer that divides the landscape by similarity of soil and climatic conditions. We developed the initial communities layer by dividing the landscape into a 150m grid and assigning species age-cohorts to each grid cell using U.S. Forest Service Forest Inventory and Analysis (FIA) plot data from 2000-2010 (O' Connell *et al.*, 2013, see Supplemental Material). The initial communities layer included 24 tree species (Table S1), which represented 95% of the individual trees in the FIA data within our study area. We divided the study area into 18 ecoregions (Fig. 1) using the U.S. Forest Service Ecological Provinces and Sections map (Cleland *et al.*, 2007) and the U.S. Environmental Protection Agency level IV ecoregion map (U.S. EPA, 2013) to capture general patterns of vegetation, climate, and soil type and facilitate parameterization of the extensions.

The Century extension was derived from the original CENTURY soil model and simulates pools and fluxes of carbon and nitrogen (Metherell *et al.*, 1993; Parton *et al.*, 1993). Cohort growth, defined by species and functional group level parameters, is influenced by soil characteristics (e.g., soil texture) and climate inputs. Recruitment of new cohorts is determined by minimum January temperature, growing degree days, and species-level tolerance of drought and shade, factors that vary as a function of climate. Cohorts compete for resources and growing space within each grid cell and disperse across grid cells, leading to changes in species distributions. Non-disturbance mortality occurs as cohorts mature (e.g., the stem-exclusion phase) and approach their maximum age. Climate extreme-induced mortality (e.g., large tree dieback events) is not currently included in the model (see Discussion). Fire-induced mortality results in the majority of the live tree C being transferred to the dead C pool, with a small fraction being volatilized to the atmosphere as a function of the fire severity.

Century requires parameters for species and functional groups and ecoregion-level soil and climate data to model recruitment and growth response. Species and functional group parameters were gathered from the literature, online sources, or estimated following algorithms in LANDIS-II (see Supplemental Material and Tables S2-S3). Soil properties such as soil texture, drainage class, and initial pools of C and nitrogen (N) were developed as a spatially-weighted average to 1 m soil depth for each ecoregion (Tables S4-S5) using the NRCS gSSURGO database (NRCS, 2013) following the methodology outlined in CENTURY model documentation (Metherell *et al.*, 1993). Soil organic matter decay rates were estimated based on Schimel *et al.* (1994) and calibrated following Loudermilk *et al.* (2013). Century uses means and standard deviations of monthly temperature and precipitation to create distributions for drawing monthly climate data for driving simulations. For this

study climate distributions were developed using downscaled (12km) climate projections (see Climate Scenarios). Climate inputs were at the same scale as the 12 km climate projection grids which best retain the spatial variability of climate over the landscape. The extension does not include CO<sub>2</sub> fertilization effects, which can increase water use efficiency (Keenan *et al.*, 2013). However, sustained CO<sub>2</sub> fertilization effects are less likely due to N limitation (Norby *et al.*, 2010), as nitrogen inputs in the Sierra Nevada are relatively small (Fenn *et al.*, 2003).

We used the Dynamic Fuel extension to assign fuel types based on vegetation characteristics to each 150m grid cell. The fuel type parameterization represents general fuel conditions and influences the rate of spread and fire severity when wildfire is simulated. Fuel type is dynamic and the fuel type for a specific grid cell is reassigned at each time step as a function of species composition and age and the occurrence of disturbance at the previous time step. We developed seventeen fuel types (Table S6) by binning general forest types that burn in a similar manner following previous work conducted in the southern Sierra Nevada (Spencer *et al.*, 2008; Sturtevant *et al.*, 2009; Syphard *et al.*, 2011).

We used the Dynamic Fire extension to simulate stochastic wildfire events. Working in conjunction with Dynamic Fuels, this extension simulates fire behavior (e.g., fire spread) and effects (e.g., cohort mortality) based on fuel types, fire weather and topographic data using a methodology similar to the Canadian Forest Fire Behavior Prediction System (Van Wagner et al., 1992). The occurrence of a fire is determined based on the probability of ignition. Fire size is randomly drawn from a user-defined fire size distribution. Fire spread/shape is determined based on minimum travel time across pixels given fuel conditions, fire weather, and topography. The topography-adjusted fire spread rate is calculated based on slope and aspect layers following equations from Van Wagner (1987). Fire weather data associated with a fire event is randomly selected from a distribution of fire weather data following the assumption that larger fires tend to occur when fire weather is more favorable for burning (e.g., higher temperature, lower fuel moisture). Simulated wildfires reach varying levels of fire severity given the complex interactions among fuels, weather and topography. Actual severity (e.g., cohorts killed) depends on both cohort age and species-specific fire tolerance relative to the severity of a fire (e.g., the youngest cohorts with low fire tolerance are most vulnerable).

Following Syphard *et al.* (2011), we stratified the study area into three fire regions (Fig. S1b) using digital elevation model (DEM) data to broadly reflect fire regime attributes, including fire size distribution and fire frequency, that correspond to the low-elevation dry forests and woodlands (<1190m), mid-elevation mixed-conifer forests (1190-2120m), and upper montane and subalpine forests (>2120m). Fire size distributions were constructed using climate projection specific large wildfire projections (>200 ha, see Wildfire Scenarios). Ignition frequency was parameterized and calibrated for each fire region based on contemporary wildfire records (http://frap.fire.ca.gov/). Representative fire weather inputs, including daily values of wind speed, wind direction, fine fuel moisture, and buildup index were obtained using Fire Family Plus 4.1 (Bradshaw & McCormick, 2000), based on daily weather records (e.g., temperature, relative humidity, precipitation, wind speed and direction, etc.) from selected Remote Automatic Weather Stations (RAWS, Fig. S1b). We used RAWS data from stations that had the most complete fire season records for the period 2000-2013 to develop the fire weather distributions, a date range that is characterized by an upward trend of high to extreme fire danger days (Collins, 2014). Spatial layers of slope and aspect data (150m resolution) were obtained from LANDFIRE (http://www.landfire.gov). Fuel-specific

spread parameters (Table S6) were calibrated based on spread rates in Scott & Burgan (2005) and fire severity distributions of fire-regime types in Thode *et al.* (2011).

### Model validation

We compared populated initial communities and simulated aboveground C (AGC) to data obtained from FIA data and other empirical-based estimates (Kellndorfer *et al.*, 2011; Wilson *et al.*, 2013; Gonzalez *et al.*, 2015). The spatial distribution of forest types in the initial communities layer represented the spatial distribution of forest types in FIA plots across the study area (Fig. S3). Simulated mean AGC was obtained following model spin-up (where forest communities are grown to their parameterized ages, representing a current condition of the forested landscape). FIA plot-level AGC estimates were scaled from individual tree biomass calculated using genus-specific allometric equations from Jenkins *et al.* (2003). The simulated AGC exhibited much of the same variability as the empirical-based estimates, although the ranges of extreme values were not fully captured due to the difference in the scale between our simulation and empirical-based estimates (Fig. S4). However, as parameterized, the model captured the influence of species composition and age structure, as well as climate and site conditions on forest productivity.

### Climate Scenarios

We used downscaled (12 km) Intergovernmental Panel on Climate Change Fourth Assessment Report (IPCC, 2007) climate projections (Hidalgo et al., 2008; Maurer & Hidalgo, 2008) from three general circulation models (GCMs), forced by the business-asusual (A2) emission scenario to develop monthly temperature and precipitation distributions from 2010 to 2100 for use in LANDIS-II. We used the GCM data to calculate monthly means and standard deviations of temperature and precipitation for each decade of the simulation period. We used the historical period (1980-2010) of the GCM data to develop baseline monthly climate distributions specific to each GCM. The three GCMs were selected from a suite of GCMs evaluated for California by Cayan et al. (2009) on the basis of their fidelity in capturing climate variability and seasonality over the historical period. The selected GCMs were as follows: GFDL CM2.1 (GFDL, Geophysical Fluid Dynamics Lab coupled model); NCAR CCSM3 (CCSM3, National Center for Atmospheric Research Community Climate System Model); CNRM CM3 (CNRM, Centre National de Recherches Météorologiques Coupled Global Climate Model). Across the study area, all GCM projections showed a warming trend throughout the simulation period (2010-2100), with CNRM having the largest increase in late-century temperature (Fig. S5). Precipitation was more variable between the different GCM projections. During early 21st century, the water budget (water balance between precipitation and potential evapotranspiration, a proxy indicating water available to plants) was highly variable between GCMs (Fig. S6). However, by late-century the water budget associated with each GCM became negative at low- and mid-elevations. Projections from CNRM and GFDL had the largest reduction in water budget from early to late century.

### Wildfire Scenarios

Large wildfires that escape initial suppression effort represent a small fraction of total wildfires, but account for a disproportionately large fraction (>95%) of total area burned per year (Strauss *et al.*, 1989; Miller & Safford, 2012). Over large areas, these events are primarily influenced by climate (Turner & Romme, 1994; Westerling *et al.*, 2006; Littel *et al.*, 2009). We used GCM-specific fire size projections (12 km resolution) for large wildfires (>200 ha) developed by Westerling *et al.* (2011a) using generalized Pareto distributions of log-area burned from historical fires conditional on climate projections (cumulative monthly moisture deficit) and land surface characteristics (topography and LANDFIRE fire regime

condition class). We used these fire size projection data for all 12 km grid cells within each fire region to develop fire size distributions that were updated each decade from 2010 to 2100 for each fire region (Table S7). We developed baseline fire size distributions specific to each GCM using data from 1980-2010. The start of the baseline period was constrained by the availability of comprehensive FIA data to characterize biomass. However, significant climate change is already represented in observations and simulations for the 1980-2010 period, so comparisons between the baseline and later simulations understate the full impact of climate change on wildfire in Sierran forests. Furthermore, since we are only simulating large wildfires, we are making the inherent assumption that fire suppression effectiveness will remain consistent in the future. All fire parameters, with the exception of fire size distributions, were held constant between scenarios. Simulations that included projected wildfire resulted in increased mean fire size and area burned and decreased fire rotation relative to baseline wildfire for all GCMs (Table 1, Fig. S7).

# Simulations & data analysis

We ran 90-year (2010-2100) simulations using the 150m grid and a 10-year time step for each scenario. The scenarios included baseline climate and wildfire and projected climate and wildfire for each GCM. We ran five replicate simulations for each scenario as a compromise between requisite computational time and expected stochasticity in climate and wildfire. To facilitate landscape-scale comparison between scenarios and account for the uniform climate data within each 12km grid cell, we aggregated the 150m forest simulation grid cells to the scale of the climate projections (12km) for analysis, such that the results for each 12km grid cell are the composite of 6400 individual 150m grid cells. To evaluate the change of spatial pattern in overstory and regeneration, we assigned dominant overstory or regeneration species to each 12km grid cell based on the species that most frequently had the highest biomass across replicates at late-century (2100) or had the highest number of total recruitment events across replicates over the course of the simulation. We combined total recruitment events for all species over the simulation period within each 12 km grid and calculated the mean percent change relative to baseline for each GCM across replicates. To evaluate changes in species composition, we categorized each 12 km grid with the most frequent tree species richness (count of tree species) in the nested 150m grid cells across GCMs and replicates by late-century (2100). To evaluate the effects of projected climatewildfire interactions on landscape C dynamics, we used a t-test to compare mean late-century (2100) landscape aboveground C between baseline and projected scenarios for each elevation band and calculated mean landscape net ecosystem C balance (NECB), a net C flux that included net primary productivity, respiration, and C loss from wildfire, for each elevation band over the simulation period. We used ArcMap 10.1 (ESRI, 2012) and R v3.2.2 (R Core Team, 2015) to conduct analyses and produce figures.

### Results

By late-century, we found modest changes in the spatial distribution of dominant species by biomass relative to the baseline scenarios (Fig. 2a, b). The change primarily occurred on the west slope of the Sierra Nevada at lower elevations, with a 15% decrease in the spatial extent of white fir, Douglas-fir and incense-cedar dominated forests and a 17% increase in the spatial extent of oak-dominated forest as well as a slight increase (2%) in the spatial extent of ponderosa pine dominated forests. The spatial extent of red fir dominated forests increased by 18% at mid elevations and by 5% at higher elevations. The change on the eastern slope was moderate because the spatial scale of the climate data (12 km) covers a large range of elevation on this much steeper elevation gradient. Changes in dominant species varied little between GCMs (Fig. S8).

In contrast to the modest changes in dominant species by biomass, we found an extensive reduction in recruitment relative to baseline over the entire landscape (Fig. S9). Across GCMs and elevation bands, 28% to 91% of the landscape experienced a greater than 50% reduction in total recruitment events during the simulation period (Table 2). The reduction in recruitment events was primarily in the low and mid-elevation bands. We did find an increase in recruitment events in some areas of the high-elevation band (>2120 m). The decline in recruitment events was largest under the drier GFDL and CNRM climate projections (Table 2 and Fig. S9).

Although forest recruitment declined across much of the Sierra, we found that projected climate and wildfire favored the recruitment of more drought-tolerant species relative to baseline (Fig. 2c, d). In the lowest elevation band (< 1190 m), the number of grid cells where gray pine had the largest number of new cohorts increased by 11% along the western slope, while the proportion of the lowest elevation band where ponderosa pine had the most new cohorts decreased by 17%. In the mid-elevation band (1190-2120 m), where we had hypothesized the largest changes in species recruitment, we found marked increases in the spatial extent where recruitment was dominated by ponderosa pine (16%), pinyon pine (21%) and oaks (267%) and a reduction in the spatial extent where recruitment was dominated by white fir, Douglas-fir and incense-cedar (-83%). In the highest elevation band, the spatial extent where Jeffrey pine had the largest number of recruits increased by 13% and pinyon pine increased by 56%, while the spatial extent where red fir (-50%) and subalpine species (-9%) had the largest number of recruits decreased. Expansion of pinyon pine recruits occurred along the east side of the Sierra Nevada and in the southern end of the mountain range. While currently present in the southern Sierra Nevada, the expansion of pinyon pine regeneration across this area may be a function of our simulations not including shrub species, which can remain dominant at a site with more frequent fire occurrence (Keeley et al., 2005). Shifts in the distribution of recruits towards more drought-tolerant species were largest under the GFDL and CNRM climate projections (Fig. S10).

With projected climate and wildfire limiting recruitment, we found a substantial reduction in tree species richness within each elevation band by late-century relative to baseline (Fig. 3). Overall, the spatial extent of low-richness communities (<3 species) increased by 37% while higher-richness communities (>6 species) decreased by 44%. The largest declines in species richness were in the mid-elevation band. Changes in species richness varied little between GCMs (Fig. S11).

As forests matured, NECB declined under all climate scenarios and across all elevation bands. However, projected changes in climate and wildfire caused a sharper decline in NECB relative to baseline (Fig. 4), with more than 80% of the study area experiencing a decline in the sink strength by late-century (Fig. S12). Although the study area remained a C sink (NECB>0) throughout all simulations, by late-century, a greater percentage of the study area became a C source (Fig. 5) and aboveground C decreased significantly relative to baseline at low (p<0.01) and mid (p<0.01) elevations (Fig. 2b). While the reduction in C on a per unit area basis was relatively small (Fig. S13), across the Sierra Nevada it equated to an average of 1.7 Tg C reduction in the low-elevation band and 4.1 Tg C reduction in the mid-elevation band by late-century. The reductions in aboveground C relative to baseline were largest under the GFDL and CNRM climate projections (Fig. S8).

Discussion

Projected changes in climate are expected to cause changes in species distributions as they move to track their appropriate climate space. Biome-based simulations of vegetation response to changing climate suggest a substantial displacement of vegetation types across the Sierra Nevada under future climate, with a marked spatial contraction of subalpine forests and displacement of mixed-conifer forests by other vegetation types (Hayhoe *et al.*, 2004; Lenihan *et al.*, 2008). However, our results did not show appreciable change in the spatial distribution of forest species cover at mid and high elevations (Fig. 2a, b), suggesting there might be a lag effect in vegetation adjustment to environmental change (Williams *et al.*, 2007; Bertrand *et al.*, 2011; Dolanc *et al.*, 2013; Svenning & Sandel, 2013). Conifer species in the Sierra Nevada are mostly long-lived. Except for extreme events, such as drought-induced forest dieback (McIntyre *et al.*, 2015) and stand-replacing fires, mature individuals are able to endure significant environmental change (Eriksson, 1996; Morris *et al.*, 2008; Dolanc *et al.*, 2013), requiring several decades to centuries for up-slope migration of species distributions to be fully realized.

Because tree seedlings tolerate a more constrained range of abiotic conditions than mature trees (Jackson et al., 2009; Mok et al., 2012), we had predicted larger changes in recruitment than in overstory species under projected climate and wildfire scenarios. We found both a large decrease in recruitment events (Table 2 and Fig. S9) and that the spatial distribution of species-specific regeneration was considerably more sensitive to projected climate and wildfire scenarios than overstory species (Fig. 2). The decrease in recruitment events occurred primarily at low- and mid-elevations due to increased moisture limitation (Table 2 and Fig. S6). The extensive reduction of recruitment can affect species abundance and may increase species' extinction risk due to extreme events, such as hotter drought (Lloret et al., 2004; Thomas et al., 2004; Allen et al., 2015). Where previous biome-based modeling efforts found significant impacts of climate change on high-elevation vegetation (Lenihan et al., 2008), we found an increase in recruitment events at many of the highest elevation areas (Table 2 and Fig. S9). This may be caused by a beneficial effect from warming temperature at high elevation sites where precipitation is non-limiting under projected climate. Recent empirical research found that warming temperature in non-moisture limited systems alleviated the climatic stress for recruits and led to relatively abundant and frequent regeneration (Dodson & Root, 2013; Dolanc et al., 2013).

We hypothesized that changing climate and wildfire would favor the recruitment of drought-tolerant species over drought-intolerant species and this change would be greatest at midelevations. Although projected climate and wildfire decreased forest recruitment across much of the Sierra Nevada, species with relatively higher drought tolerance (e.g., oak, gray pine, ponderosa pine, pinyon pine, and Jeffrey pine) accounted for the majority of recruits (Fig. 2c, d). Species that are less drought-tolerant (e.g., white fir, Douglas-fir, and red fir) had recruitment events that were disproportionately less than their contribution to overstory abundance under projected climate and wildfire. These species-specific shifts in recruitment were largest at mid-elevations where less drought-tolerant species (e.g., white fir) had proliferated during the 20<sup>th</sup> century due to fire suppression (McKelvey *et al.*, 1996; Scholl & Taylor, 2010). These trends are consistent with recent empirical studies that documented significant thermophilization in forest understory as facilitated by climate warming and wildfires (De Frenne *et al.*, 2013; Stevens *et al.*, 2015). The altered recruitment distribution may initiate cascading effects on forest successional trajectory, affecting community composition and species abundance in the long term (Grubb, 1977; Lloret *et al.*, 2004).

Given our prediction for projected climate and wildfire to have a larger impact on tree regeneration, we hypothesized that tree species richness would decline by late-century. We found the decrease in recruitment under projected climate and wildfire led to an increased proportion of the landscape having lower tree species richness (Fig. 3). Simplified community composition and a shift toward more drought-tolerant recruitment suggest that species that are least tolerant to environmental change may be unable to establish under projected future conditions. The simplification of forest communities could impact forest productivity as well as C sequestration (Chapin III et al., 2000; Cardinale et al., 2012). Forests with lower tree species richness are also more vulnerable to insect and pathogen outbreaks (Dale et al., 2001). Bark beetles, defoliators, and plant disease all tend to be hostspecific at the level of tree genus (Hicke et al., 2012). Given the current level of insectinduced mortality in low-elevation pines in the Southern Sierra Nevada (Potter, 2016), increasing outbreaks of these biotic disturbances in a simpler, pine-dominated forest community (Fig. 2, Fig. 3) under climate change may cause substantial tree mortality and exert profound impacts on the integrity and functioning of forest ecosystems (Brown et al., 2010; Hicke et al., 2013; Ghimire et al., 2015).

Large-scale forest disturbances pose a risk to the provision of ecosystem services (Millar & Stephenson, 2015). We hypothesized that projected climate and increasing burned area would drive an increase in the proportion of the landscape that is a C source because larger fires and increasing extent of high-severity burn patches have been found to slow or limit post-fire forest recovery due to dispersal limitation and drought stress (Collins & Roller, 2013; Dodson & Root, 2013; Stephens *et al.*, 2013), factors that could more extensively impact Sierran forests with warming climate and increasing area burned. Our results of declining NECB, reduced aboveground C, and a greater proportion of landscape being a C source by late-century under projected climate and wildfire suggest that the combined effects of these global change factors and the resultant changes in forest community composition will impact forest C dynamics. The result of increasing area becoming a C source also implicitly demonstrates the potential for an altered successional pathway with burned area transitioning to a lower C state following high-severity wildfire.

Our simulation approach is limited by four factors, changing fire regimes, excluding shrub species, extreme drought-induced tree mortality, and the coarse scale of the projected climate data, all of which could impact the results. Our simulations only included climate-driven increases in wildfire size and therefore are a conservative estimate of projected wildfire impacts on forests. Given the influence of changing climate and increasing area burned on the number of regeneration events, species-specific regeneration success, and C dynamics in the system, the potential exists for additional impacts with changes in other aspects of fire regimes. Wildfire is expected to become more frequent due to both climate change and human activities (Syphard et al., 2007; Lutz et al., 2009; Moritz et al., 2012). As extreme wildfire weather becomes more common under warming climate (Collins, 2014), increasing area burned is likely to be accompanied by an increase in the area impacted by high-severity wildfire (Dillon et al., 2011; Westerling et al., 2011a; Miller & Safford, 2012; Harris & Taylor, 2015). The increasing frequency of extreme fire weather may also lead to diminished fire suppression effectiveness, thus resulting in more large wildfires. Realization of climatedriven changes in all elements of fire regimes (e.g., frequency, severity) may increase fireinduced tree mortality and post-fire C release (Kashian et al., 2006; Dore et al., 2008; North & Hurteau, 2011; van Mantgem et al., 2013), which could accelerate tree species shifts and cause further decline in the C sink strength. Furthermore, because our simulations did not include shrub species, our results represent a conservative estimate of vegetation shift from

tree dominated to shrub dominated communities following high-severity wildfire. Previous studies show that shrubs are often fire-adapted and reestablish quickly in large high-severity burn patches (Kauffman & Martin, 1991; Knapp *et al.*, 2012). Once established, a positive feedback loop can form with subsequent fires to reinforce a shrub dominated community and reduce tree regeneration (Odion *et al.*, 2010; Coppoletta *et al.*, 2016; Lauvaux *et al.*, 2016). This dynamic, in addition to environmental stress, may further limit forest development and result in larger areas being type converted from tree dominated to shrub dominated in severely burned stands. Thus, competition from non-tree species may likely restrain the expansion of pinyon pine on the eastside and southern Sierra where chaparral communities are persistent.

Tree mortality and forest dieback are likely to accelerate with rising temperature and accompanying drought because the atmospheric water demand during periods of high vapor pressure deficit can cause hydraulic failure (Adams et al., 2009; Williams et al., 2012; Allen et al., 2015; McDowell et al., 2016). In addition, increasing drought stress can facilitate insect outbreaks by weakening the natural defenses of host trees, thereby leading to widespread conifer mortality (Kurz et al., 2008; Ghimire et al., 2015). Because our model does not capture the mechanistic process of cavitation during extreme drought and we did not simulate insect outbreaks, our results may overstate the climate resilience of Sierran forests and increasing extreme drought frequency could cause faster change of overstory species. Widespread, climate-induced tree mortality events would not only impact species distributions, but would also negatively impact NECB and aboveground C. While additional investigation is needed to better understand how this type of event will influence Sierran forests, these ecosystems are unlikely to be uniformly impacted because topographic heterogeneity can mediate climate and buffer forests from direct climate impacts (Loarie et al., 2009; Dobrowski, 2011; Franklin et al., 2013). However, our ability to simulate the influence of topography on climate variability is currently limited by the scale of the projected climate data. As an example, the eastern slope of the Sierra Nevada has a steep elevation gradient and a wide range of elevations are simulated with the same climate because they fall within a 12 km climate grid cell. Thus, climate for lower elevation woodlands and higher elevation forests were drawn from the same monthly distributions. The resolution of the projected climate data could drive an overestimate of the potential expansion of woodland species, such as pinyon pine, and a decline of higher elevation species. Furthermore, this resolution precludes climate variability as a function of topographic features within a projected climate grid cell. Efforts to further downscale climate projections over the Sierra Nevada are underway (Flint & Flint, 2012) and could improve the ability to simulate species movement in this topographically complex landscape.

Our results are also impacted by assumptions stemming from model structure uncertainty. In LANDIS-II, the set relationships between species performance (e.g., species recruitment and vegetative growth) and environmental factors (e.g., CO<sub>2</sub>, moisture, and fire severity) are assumed to be unchanged over time. Under climate change, these relationships may be altered due to species acclimation or maladaptation responses (Keenan *et al.*, 2013; van Mantgem *et al.*, 2013). The model assumes that species phenological activities are unaffected by climate warming. However, increasing temperature may shift species phenology and undermine the conditions required for species development (e.g., pre-chilling for germination), thus affecting subsequent species growth (Memmott *et al.*, 2007; Harrington *et al.*, 2010). Forest response to climate and wildfire is a complex, multiscale process, which is difficult to study at large spatio-temporal scales using empirical approaches. Thus, while forest landscape models, such as LANDIS-II, require assumptions and include model

structure uncertainty, by taking account of spatial interactions of multiple ecological processes, they provide a realistic and heuristic tool to study forest landscape response.

Across the Sierra Nevada, our simulations showed disparate responses in overstory dominant species and understory recruitment to environmental change. Over the 21<sup>st</sup> Century, forest communities are unlikely to diminish as intact units as predicted by biome-based modeling, but are likely to trend toward simplified community composition as communities gradually disaggregate and the least tolerant species are lost. Furthermore, our results of reduced species richness and altered recruitment distribution suggest there is great potential for community composition change and forest simplification beyond this century. However, this change could accelerate with climate-driven forest dieback, related insect outbreaks and increasing fire frequency. Our results highlight the importance of accounting for species-specific dynamics in landscape modeling and suggest higher resolution climate projections are necessary to better capture the influence of topographically-mediated climate on species distributions. We should expect similar mechanisms of response to environmental change in other Mediterranean and semi-arid mountain ranges worldwide, where interspecific differences, topography, and disturbance influence forest community composition and productivity.

### Acknowledgements

This work was supported by the National Institute of Food and Agriculture, U.S. Department of Agriculture, under grant number GRANT11026720. We thank Melissa Lucash, Megan Creutzburg and Louise Loudermilk for help with model parameterization and Jeanne Milostan for providing data support. We also thank the LANDIS-II User Group for help throughout this study and the anonymous reviewers who provided helpful feedback on an earlier version of this manuscript.

### References

Adams HD, Guardiola-Claramonte M, Barron-Gafford GA, Camilo Villegas J, Breshears DD, Zou CB, Troch PA, Huxman TE (2009) Temperature sensitivity of drought-induced tree mortality portends increased regional die-off under global-change-type drought. *Proceedings of the National Academy of Sciences*, **106**, 7063-7066.

Allen CD, Breshears DD, McDowell NG (2015) On underestimation of global vulnerability to tree mortality and forest die-off from hotter drought in the Anthropocene. *Ecosphere*, **6**, 1-55.

Bachelet D, Neilson RP, Lenihan JM, Drapek RJ (2001) Climate change effects on vegetation distribution and carbon budget in the United States. *Ecosystems*, **4**, 164–185.

Bertrand R, Lenoir J, Piedallu C *et al.* (2011) Changes in plant community composition lag behind climate warming in lowland forests. *Nature*, **479**, 517–520.

Bradshaw LS, McCormick E (2000) *FireFamily Plus user's guide, Version 2.0.* General Technical Reports RMRS-GTR-67WWW, USDA Forest Service, Rocky Mountain Research Station, Ogden, UT.

Brown M, Black TA, Nesic Z *et al.* (2010) Impact of mountain pine beetle on the net ecosystem production of lodgepole pine stands in British Columbia. *Agricultural and Forest Meteorology*, **150**, 254–264.

Cardinale BJ, Duffy JE, Gonzalez A *et al.* (2012) Corrigendum: Biodiversity loss and its impact on humanity. *Nature*, **489**, 326–326.

Cayan D, Tyree M, Dettinger M et al. (2009) Climate change scenarios and sea level rise estimates for the California 2009 Climate Change Scenarios Assessment. California Energy

Commission Report CEC-500-2009-014-D, California Climate Change Center, Sacramento, CA.

Chapin FS, Zavaleta ES, Eviner VT *et al.* (2000) Consequences of changing biodiversity. *Nature*, **405**, 234–42.

Cleland DT, Freeouf JA, Keys JE, Nowacki GJ, Carpenter CA, McNab WH (2007)

 $Ecological\ subregions:\ sections\ and\ subsections\ for\ the\ conterminous\ United\ States.\ U.S.$ 

Department of Agriculture, Forest Service, Washington, DC, Map scale, 1:3,500,000.

Collins BM (2014) Fire weather and large fire potential in the northern Sierra Nevada. *Agricultural and Forest Meteorology*, **189**, 30–35.

Collins BM, Roller GB (2013) Early forest dynamics in stand-replacing fire patches in the northern Sierra Nevada, California, USA. *Landscape Ecology*, **28**, 1801–1813.

Coppoletta M, Merriam KE, Collins BM (2016) Post-fire vegetation and fuel development influences fire severity patterns in reburns. *Ecological Applications*, **26**, 686-699.

Dale VH, Joyce LA, Mcnulty S *et al.* (2001) Climate Change and Forest Disturbances. *BioScience*, **51**, 723–734.

De Frenne P, Rodriguez-Sanchez F, Coomes DA *et al.* (2013) Microclimate moderates plant responses to macroclimate warming. *Proceedings of the National Academy of Sciences*, **110**, 18561–18565.

Dillon GK, Holden AZ, Morgan P, Crimmins MA, Heyerdahl EK, Luce CH (2011) Both topography and climate affected forest and woodland burn severity in two regions of the western US, 1984 to 2006. *Ecosphere*, **2**, 1-33.

Dobrowski SZ (2011) A climatic basis for microrefugia: the influence of terrain on climate. *Global Change Biology*, **17**, 1022-1035.

Dobrowski SZ, Abatzoglou J, Swanson AK, Greenberg JA, Mynsberge AR, Holden ZA, Schwartz MK (2013) The climate velocity of the contiguous United States during the 20th Century. *Global Change Biology*, **19**, 241-251.

Dodson EK, Root HT (2013) Conifer regeneration following stand-replacing wildfire varies along an elevation gradient in a ponderosa pine forest, Oregon, USA. *Forest Ecology and Management*, **302**, 163–170.

Dolanc CR, Thorne JH, Safford HD (2013) Widespread shifts in the demographic structure of subalpine forests in the Sierra Nevada, California, 1934 to 2007. *Global Ecology and Biogeography*, **22**, 264–276.

Dore S, Kolb TE, Montes-Helu M *et al.* (2008) Long-term impact of a stand-replacing fire on ecosystem CO2 exchange of a ponderosa pine forest. *Global Change Biology*, **14**, 1801–1820.

Eriksson (1996) Regional Dynamics of Plants: A Review of Evidence for Remnant, Source-Sink and Metapopulations. *Oikos*, **77**, 248–258.

ESRI (2012) ArcMap desktop. Release 10.1. Environmental Systems Research Institute, Redlands, CA, USA.

Fenn ME, Poth MA, Bytnerowicz A, Sickman JO, Takemoto BK (2003) Effects of ozone, nitrogen deposition, and other stressors on montane ecosystems in the Sierra Nevada. *Developments in Environmental Science*, **2**, 111–155.

Flint LE, Flint AL (2012) Downscaling future climate scenarios to fine scales for hydrologic and ecological modeling and analysis. *Ecological Processes*, **1**, 2, doi: 10.1186/2192-1709-1-2.

Franklin J, Davis FW, Ikegami M, Syphard AD, Flint LE, Flint AL, Hannah L (2013) Modeling plant species distributions under future climates: how fine scale do climate projections need to be? *Global Change Biology*, **19**, 473–83.

Ghimire B, Williams CA, Collatz GJ, Vanderhoof M, Rogan J, Kulakowski D, Masek JG (2015) Large carbon release legacy from bark beetle outbreaks across Western United States. *Global Change Biology*, **21**, 3087-101.

Gill L, Taylor AH (2009) Top-down and bottom-up controls on fire regimes along an elevational gradient on the east slope of the Sierra Nevada, California, USA. *Fire Ecology*, **5**, 57–75.

Gonzalez P, Neilson RP, Lenihan JM, Drapek RJ (2010) Global patterns in the vulnerability of ecosystems to vegetation shifts due to climate change. *Global Ecology and Biogeography*, **19**, 755–768.

Gonzalez P, Battles JJ, Collins BM, Robards T, Saah DS (2015) Aboveground live carbon stock changes of California wildland ecosystems, 2001–2010. *Forest Ecology and Management*, **348**, 68–77.

Grubb PJ (1977) The Maintenance of Species-Richness in Plant Communities: the Importance of the Regeneration Niche. *Biological Reviews*, **52**, 107–145.

Harrington CA, Gould PJ, St Clair JB (2010) Modeling the effects of winter environment on dormancy release of Douglas-fir. *Forest Ecology and Management*, **259**, 798-808.

Harris L, Taylor AH (2015) Topography, fuels, and fire exclusion drive fire severity of the Rim Fire in an old-growth mixed-conifer forest, Yosemite National Park, USA. *Ecosystems*, **18**, 1192-1208.

Hayhoe K, Cayan D, Field CB *et al.* (2004) Emissions pathways, climate change, and impacts on California. *Proceedings of the National Academy of Sciences of the United States of America*, **101**, 12422–7.

Heyerdahl EK, Morgan P, Riser JP (2008a) Multi-season climate synchronized historical fires in dry forests (1650–1900), northern Rockies, USA. *Ecology*, **89**, 705-716.

Heyerdahl EK, McKenzie D, Daniels LD, Hessl AE, Littell JS, Mantua NJ (2008b) Climate drivers of regionally synchronous fires in the inland Northwest (1651–1900). *International Journal of Wildland Fire*, **17**, 40-49.

Hicke JA, Allen CD, Desai AR *et al.* (2012) Effects of biotic disturbances on forest carbon cycling in the United States and Canada. *Global Change Biology*, **18**, 7–34.

Hicke JA, Meddens AJH, Allen CD, Kolden CA (2013) Carbon stocks of trees killed by bark beetles and wildfire in the western United States. *Environmental Research Letters*, **8**, 035032.

Hidalgo HG, Dettinger MD, Cayan DR (2008) Downscaling with Constructed Analogues:

Daily Precipitation and Temperature Fields over the United States. California Energy Commission PIER Energy-Related Environmental Research. CEC-500-2007-123.

Hirsch KJ (1996) Canadian forest fire behavior prediction (FBP) system: user's guide.

Natural Resources Canada, Canadian Forest Service, Northwest Region, Northern Forestry Centre, Edmonton, Alberta, Special Report 7.

Hurteau MD, Brooks ML (2011) Short- and Long-term Effects of Fire on Carbon in US Dry Temperate Forest Systems. *BioScience*, **61**, 139–146.

IPCC (2007) *Climate Change 2007: The Physical Science Basis. Contribution of* Working Group I to the Fourth Assessment Report of the Intergovernmental Panel on Climate Change. Cambridge University Press, Cambridge, UK.

Jenkins JC, Chojnacky DC, Heath LS, Birdsey RA. (2003) National-scale biomass estimators for United States tree species. *Forest Science*, **49**, 12–35.

Jones C, Lowe J, Liddicoat S, Betts R (2009) Committed terrestrial ecosystem changes due to climate change. *Nature Geoscience*, **2**, 484–487.

Kashian DM, Romme WH, Tinker DB, Turner MG, Ryan MG (2006) Carbon storage on landscapes with stand-replacing fires. *BioScience*, **56**, 598–606.

Kauffman JB, Martin RE (1991) Sprouting shrub response to different seasons and fuel consumption levels of prescribed fire in Sierra Nevada mixed conifer ecosystems. *Forest Science*, **36**, 748–764.

Keeley JE, Pfaff AH, Safford HD (2005) Fire suppression impacts on postfire recovery of Sierra Nevada chaparral shrublands. International Journal of Wildland Fire, **14**, 255-265. Keenan TF, Hollinger DY, Bohrer G, Dragoni D, Munger JW, Schmid HP, Richardson AD (2013) Increase in forest water-use efficiency as atmospheric carbon dioxide concentrations rise. *Nature*, **499**, 324–7.

Kellndorfer J, Walker W, LaPoint L *et al.* (2011) NACP aboveground biomass and carbon baseline data (NBCD 2000), USA, 2000. Data set. ORNL DAAC, Oak Ridge, Tennessee. Available online at daac. ornl. gov.

Knapp EE, Weatherspoon CP, Skinner CN (2012) Shrub seed banks in mixed conifer forests of northern California and the role of fire in regulating abundance. *Fire Ecology*, **8**, 32–48. LANDFIRE (2010) Homepage of the LANDFIRE Project, U.S. Department of Agriculture, Forest Service, U.S. Department of Interior. Available online at http://www.landfire.gov. Accessed January 2013.

Lauvaux CA, Skinner CN, Taylor AH (2016) High severity fire and mixed conifer forest-chaparral dynamics in the southern Cascade Range, USA. *Forest Ecology and Management*, **363**, 74-85.

Lenihan JM, Bachelet D, Neilson RP, Drapek R (2008) Response of vegetation distribution, ecosystem productivity, and fire to climate change scenarios for California. *Climatic Change*, **87**, 215–230.

Littell JS, McKenzie D, Peterson DL, Westerling AL (2009) Climate and wildfire area burned in western U.S. ecoprovinces, 1916–2003. *Ecological Applications*, **19**, 1003–1021. Loarie SR, Duffy PB, Hamilton H, Asner GP, Field CB, Ackerly DD (2009) The velocity of climate change. *Nature*, **462**, 1052–1055.

Loudermilk EL, Scheller RM, Weisberg PJ, Yang J, Dilts TE, Karam SL, Skinner C (2013) Carbon dynamics in the future forest: The importance of long-term successional legacy and climate-fire interactions. *Global Change Biology*, **19**, 3502–3515.

Lutz JA, van Wagtendonk JW, Thode AE, Miller JD, Franklin JF (2009) Climate, lightning ignitions, and fire severity in Yosemite National Park, California, USA. *International Journal of Wildland Fire*, **18**, 765–774.

Lutz JA, van Wagtendonk JW, Franklin JF (2010) Climatic water deficit, tree species ranges, and climate change in Yosemite National Park. *Journal of Biogeography*, **37**, 936–950. Maurer EP, Hidalgo HG (2008) Utility of daily vs. monthly large-scale climate data: an intercomparison of two statistical downscaling methods. *Hydrology and Earth System Sciences*, **12**, 551–563.

McDowell NG, Williams AP, Xu C *et al.* (2016) Multi-scale predictions of massive conifer mortality due to chronic temperature rise. *Nature Climate Change*, **6**, 295–300.

McKelvey KS, Skinner CN, Chang C *et al.* (1996) An overview of fire in the Sierra Nevada. In: *Sierra Nevada Ecosystem Project: Final Report to Congress, Vol. II. Assessments and Scientific Basis for Management Options*, pp. 1033-1040, University of California, Davis. McKenney DW, Pedlar JH, Lawrence K, Campbell K, Hutchinson MF (2007) Potential impacts of climate change on the distribution of North American trees. *Bioscience*, **57**, 939–948.

McIntyre PJ, Thorne JH, Dolanc CR, Flint AL, Flint LE, Kelly M, Ackerly DD (2015) Twentieth-century shifts in forest structure in California: Denser forests, smaller trees, and increased dominance of oaks. *Proceedings of the National Academy of Sciences*, **112**, 1458-1463.

Metherell A
environmen
CO.
Millar CI, S
megadisturb
Miller JD, S
forest fire se
Nevada, US
Miller JD, S
Modoc Plate
Mok H, Arn
and change
Australia. G
Moritz MA,
Climate cha
Morris WF,
populations
Norby RJ, V
forest produ
Academy of
North MP, I
in fuels trea
NRCS (201
Conservatio
2013.
O'Connell I
database: de

Memmott J, Craze PG, Waser NM, Price MV (2007) Global warming and the disruption of plant–pollinator interactions. *Ecology Letters*, **10**, 10–717.

Metherell AK, Harding LA, Cole CV, Parton WJ (1993) Century: Soil organic matter model environment technical documentation agroecosystem version 4.0. USDA-ARS, Fort Collins, CO.

Millar CI, Stephenson NL (2015) Temperate forest health in an era of emerging megadisturbance. *Science*, **349**, 823–826.

Miller JD, Safford HD, Crimmins M, Thode AE (2009) Quantitative evidence for increasing forest fire severity in the Sierra Nevada and southern Cascade Mountains, California and Nevada, USA. *Ecosystems*, **12**, 16-32.

Miller JD, Safford H (2012) Trends in wildfire severity: 1984 to 2010 in the Sierra Nevada, Modoc Plateau, and Southern Cascades, California, USA. *Fire Ecology*, **8**, 41–57.

Mok H, Arndt SK, Nitschke CR (2012) Modelling the potential impact of climate variability and change on species regeneration potential in the temperate forests of South-Eastern Australia. *Global Change Biology*, **18**, 1053–1072.

Moritz MA, Parisien M, Batllori E, Krawchuk MA, Van Dorn J, Ganz DJ, Hayhoe K (2012) Climate change and disruptions to global fire activity. *Ecosphere*, **3**, 1-22.

Morris WF, Pfister CA, Tuljapurkar S *et al.* (2008) Longevity can buffer plant and animal populations against changing climate variability. *Ecology*, **89**, 19–25.

Norby RJ, Warren JM, Iversen CM, Medlyn BE, McMurtrie RE (2010) CO2 enhancement of forest productivity constrained by limited nitrogen availability. *Proceedings of the National Academy of Sciences of the United States of America*, **107**, 19368–19373.

North MP, Hurteau MD (2011) High-severity wildfire effects on carbon stocks and emissions in fuels treated and untreated forest. *Forest Ecology and Management*, **261**, 1115–1120. NRCS (2013) Web Soil Survey. U.S. Department of Agriculture, Natural Resources Conservation Service. Available online at http://websoilsurvey.nrcs.usda.gov. Accessed July

O'Connell BM, LaPoint EB, Turner JA et al. (2013) The Forest Inventory and Analysis database: database description and users manual version 5.16 for Phase 2. U.S. Department of Agriculture, Forest Service, Washington, DC.

Odion DC, Moritz MA, DellaSala DA (2010) Alternative community states maintained by fire in the Klamath Mountains, USA. *Journal of Ecology*, **98**, 96-105.

Parton WJ, Scurlock JMO, Ojima DS *et al.* (1993) Observations and modeling of biomass and soil organic matter dynamics for the grassland biome worldwide. *Global Biogeochemical Cycles*, **7**, 785–809.

Potter CS (2016) Landsat Image Analysis of Tree Mortality in the Southern Sierra Nevada Region of California during the 2013-2015 Drought. *Journal of Earth Science & Climatic Change*, **14**, 342.

R Core Team (2013) R: A language and environment for statistical computing. R Foundation for Statistical Computing, Vienna, Austria. Available online at http://www.R-project.org. Roccaforte JP, Fulé PZ, Chancellor WW, Laughlin DC (2012) Woody debris and tree regeneration dynamics following severe wildfires in Arizona ponderosa pine forests. *Canadian Journal of Forest Research*, **42**, 593–604.

Scheller RM, Domingo JB, Sturtevant BR, Williams JS, Rudy A, Gustafson EJ, Mladenoff DJ (2007) Design, development, and application of LANDIS-II, a spatial landscape simulation model with flexible temporal and spatial resolution. *Ecological Modelling*, **201**, 409–419.

Scheller RM, Hua D, Bolstad PV, Birdsey RA, Mladenoff DJ (2011a) The effects of forest harvest intensity in combination with wind disturbance on carbon dynamics in Lake States Mesic Forests. *Ecological Modelling*, **222**, 144–153.

Scheller RM, van Tuyl S, Clark KL, Hom J, La Puma I (2011b) Carbon sequestration in the New Jersey Pine Barrens under different scenarios of fire management. *Ecosystems*, **14**, 987–1004.

Scherrer D, Körner C (2011) Topographically controlled thermal-habitat differentiation buffers alpine plant diversity against climate warming. *Journal of Biogeography*, **38**, 406–

Scholl AE, Taylor AH (2010) Fire regimes, forest change, and self-organization in an old-growth mixed-conifer forest, Yosemite National Park, USA. *Ecological Applications*, **20**, 362–380.

Scott JH, Burgan RE (2005) *Standard fire behavior fuel models: a comprehensive set for use with Rothermel's surface fire spread model*. General Technical Reports RMRS-GTR-153, USDA Forest Service, Rocky Mountain Research Station, Fort Collins, CO.

Spencer WD, Rustigian HL, Scheller RM, Syphard A, Strittholt J, Ward B (2008) Baseline evaluation of fisher habitat and population status, and effects of fires and fuels management on fishers in the southern Sierra Nevada. Unpublished report prepared for USDA Forest Service, Pacific Southwest Region.

Stephens SL, Agee JK, Fulé PZ, North MP, Romme WH, Swetnam TW, Turner MG (2013) Managing Forests and Fire in Changing Climates. *Science*, **342**, 41–2.

Stevens JT, Safford HD, Harrison S, Latimer AM (2015) Forest disturbance accelerates thermophilization of understory plant communities. *Journal of Ecology*, **103**, 1253-1263. Strauss D, Bednar L, Mees R (1989) Do one percent of forest fires cause ninety-nine percent of the damage? *Forest Science*, **35**, 319–328.

Sturtevant BR, Scheller RM, Miranda BR, Shinneman D, Syphard A (2009) Simulating dynamic and mixed-severity fire regimes: A process-based fire extension for LANDIS-II. *Ecological Modelling*, **220**, 3380–3393.

Sugihara NG (2006) *Fire in California's Ecosystems*. University of California Press, Berkeley, CA.

Svenning J, Sandel B (2013) Disequilibrium vegetation dynamics under future climate change. *American Journal of Botany*, **100**, 1266–1286.

Syphard AD, Radeloff VC, Keeley JE, Hawbaker TJ, Clayton MK, Stewart SI, Hammer RB (2007) Human Influence on California Fire Regimes. *Ecological Applications*, **17**, 1388–1402.

Syphard AD, Scheller RM, Ward BC, Spencer WD, Strittholt JR (2011) Simulating landscape-scale effects of fuels treatments in the Sierra Nevada, California, USA. *International Journal of Wildland Fire*, **20**, 364–383.

Taylor AH, Scholl AE (2012) Climatic and human influences on fire regimes in mixed conifer forests in Yosemite National Park, USA. *Forest Ecology and Management*, **267**, 144–156.

Thode AE, Van Wagtendonk JW, Miller JD, Quinn JF (2011) Quantifying the fire regime distributions for severity in Yosemite National Park, California, USA. *International Journal of Wildland Fire*, **20**, 223–239.

Thomas CD, Cameron A, Green RE *et al.* (2004) Extinction risk from climate change. *Nature*, **427**, 145–8.

Trouet V, Taylor AH, Wahl ER, Skinner CN, Stephens SL (2010) Fire-climate interactions in the American West since 1400 CE. *Geophysical Research Letters*, **37**, L04702.

Turner MG, Romme WH (1994) Landscape Dynamics in Crown Fire Ecosystems. *Landscape Ecology*, **9**, 59–77.

U.S. Environmental Protection Agency (2013) *Level III and IV ecoregions of the continental United States*. National Health and Environmental Effects Research Laboratory, Corvallis, OR, Map scale 1:3,000,000.

This article is protected by copyright. All rights reserved.

van Mantgem PJ, Nesmith JCB, Keifer M, Knapp EE, Flint A, Flint L (2013) Climatic stress increases forest fire severity across the western United States. *Ecology Letters*, **16**, 1151–1156.

van Wagner CE, Stocks BJ, Lawson BD, Alexander ME, Lynham TJ, McAlpine RS (1992) *Development and Structure of the Canadian Forest Fire Behavior Prediction System*. Fire Danger Group, Forestry Canada, Ottawa, Ontario.

van Wagtendonk JW, Fites-Kaufman J (2006) Sierra Nevada bioregion. In *Fire in California's Ecosystems* (eds Sugihara NG, van Wagtendonk JW, Shaffer KE, Fites-Kaufman J, Thode AE), pp. 264–294. The University of California Press, Berkeley, CA.

Westerling AL (2016) Increasing western US forest wildfire activity: sensitivity to changes in the timing of Spring. *Philosophical Transactions of the Royal Society B: Biological Sciences*, **371**, 20150178.

Westerling AL, Brown TJ, Gershunov A, Cayan DR, Dettinger MD (2003) Climate and Wildfire in the Western United States. *Bulletin of the American Meteorological Society*, **84** 595-604.

Westerling AL, Hidalgo HG, Swetnam TW (2006) Warming and Earlier Spring Increase Western U.S. Forest Wildfire Activity. *Science*, **313**, 940–943.

Westerling AL, Turner MG, Smithwick EH, Romme WH, Ryan MG (2011a) Continued warming could transform Greater Yellowstone fire regimes by mid-21st Century.

Proceedings of the National Academy of Sciences, 108, 13165-13170.

Westerling AL, Bryant BP, Preisler HK, Holmes TP, Hidalgo HG, Das T, Shrestha SR (2011b) Climate change and growth scenarios for California wildfire. *Climatic Change*, **109**, 445–463.

Williams JW, Jackson ST, Kutzbach JE (2007) Projected distributions of novel and disappearing climates by 2100 AD. *Proceedings of the National Academy of Sciences of the United States of America*, **104**, 5738–5742.

Williams AP, Allen CD, Macalady AK *et al.* (2012) Temperature as a potent driver of regional forest drought stress and tree mortality. *Nature Climate Change*, **3**, 292–297. Wilson BT, Woodall CW, Griffith DM (2013) Imputing forest carbon stock estimates from inventory plots to a nationally continuous coverage. *Carbon Balance and Management*, **8**, 1-15.

Woodward FI, Lomas MR, Kelly CK (2004) Global climate and the distribution of plant biomes. *Philosophical Transactions of the Royal Society B: Biological Sciences*, **359**, 1465–1476.

Zhu K, Woodall CW, Clark JS (2012) Failure to migrate: Lack of tree range expansion in response to climate change. *Global Change Biology*, **18**, 1042–1052.

# **Supporting Information**

Additional Supporting Information may be found in the online version of this article:

- **Figure S1.** Spatial distribution of elevation gradient and fire regions.
- Figure S2. Elevation distribution of tree species.
- Figure S3. Spatial distribution of initial communities.
- Figure S4. Comparison of simulated aboveground carbon to other estimates.
- Figure S5. Changes in temperature under projected climate.
- **Figure S6.** Changes in water budget under projected climate.
- Figure S7. Area burned per decade under baseline and projected climate.
- Figure S8. GCM-specific percentage of landscape occupied by high-biomass species.
- Figure S9. Spatial distribution of percent change in total recruitment events from baseline

**Figure S10.** GCM-specific percentage of landscape occupied by species with largest number of new cohorts.

Figure S11. GCM-specific percentage of landscape occupied by tree species richness class.

Figure S12. Spatial distribution of late-century net ecosystem carbon balance.

Figure S13. Spatial distribution of late-century aboveground carbon

**Table S1.** Species life history parameters.

**Table S2.** Species physiological parameters for Century extension.

**Table S3.** Functional type parameters for species listed in Table S1.

**Table S4.** Initial soil carbon and nitrogen parameters for Century extension.

**Table S5.** Ecoregion fixed parameters.

**Table S6.** Fuel types and associated parameters

**Table S7.** Fire size distribution parameters

#### **Tables**

**Table 1** Summary of fire output statistics. Values are mean fire size (standard deviation), mean area burned (standard deviation), and fire rotation (standard deviation) across simulation periods and replicate runs. Comparison of fire attributes was conducted using the five replicate simulations for each climate scenario and the comparison between each climate scenario and the baseline scenario was conducted using a t-test (p<0.01\*\*, p<0.05\*).

Climate	Mean	Mean Area Burned	Fire Rotation	
Scenario	Fire Size (ha)	per decade (ha)	Period (yrs.)	
Baseline	1414 (2250)	158755 (27140)	212 (11)	
GFDL	1578 (2829)**	177272 (33204)**	190 (10)**	
CCSM3	1525 (2563)	173718 (27471)*	194 (13)	
CNRM	1647 (2675)**	185393 (33235)**	182 (8)**	

**Table 2** Percentage of each elevation band characterized by each class of percent change in total recruitment events from baseline under each climate model. Total recruitment events are for all species over the simulation period. Values represent mean and standard error across five replicate simulations.

	Elevation	Scenarios	Percentage of land area (%)				
Band (m)	Scenarios	<-50%	-50% to <5%	0±5%	>5% to 50%	>50%	
	<1190	GFDL	72.1 (0.4)	24.7 (0.3)	1.0 (0.5)	2.0 (0.5)	0.2 (0.2)
		CCSM3	66.5 (0.6)	16.8 (0.7)	4.6 (1.0)	10.4 (1.4)	1.7 (0.6)
		CNRM	90.5 (1.5)	8.8 (1.3)	0.7 (0.3)	0	0
•	1190-2120	GFDL	74.6 (0.7)	19.2 (1.1)	2.0 (0.4)	2.7 (0.5)	1.5 (0.5)
		CCSM3	40.7 (0.9)	39.1 (0.4)	3.4 (0.7)	9.0 (1.1)	7.8 (0.3)
		CNRM	86.4 (1.1)	11.9 (0.8)	0.6 (0.2)	0.9 (0.3)	0.2 (0.1)
•	>2120	GFDL	58.4 (0.7)	19.3 (0.7)	1.4 (0.3)	5.9 (0.4)	15.0 (0.3)
		CCSM3	27.6 (0.6)	41.4 (1.2)	3.1 (0.5)	8.6 (0.7)	19.3 (0.3)
		CNRM	55.4 (0.6)	22.6 (0.8)	2.2 (0.5)	6.1 (0.4)	13.7 (0.5)

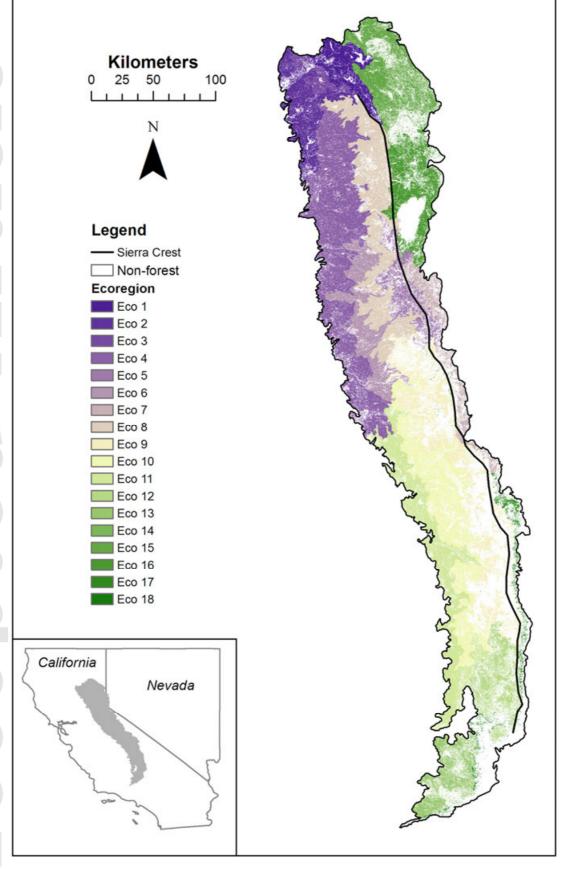
Figure Captions

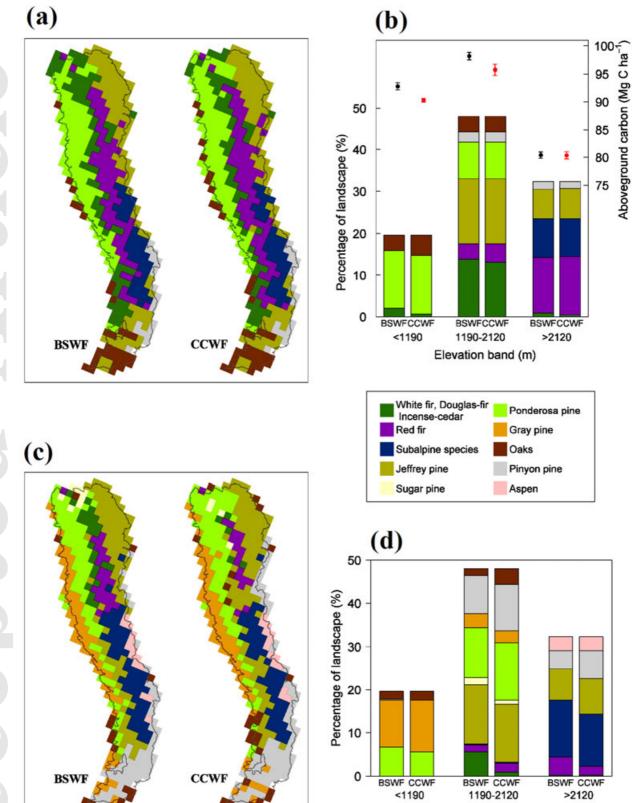
**Figure 1** Map of study area, the Sierra Nevada Mountains, CA and NV, USA. Colored background shows the eighteen ecoregions used in LANDIS-II simulations. The black line shows the approximate location of the Sierra Nevada crest, differentiating the east and west slopes.

**Figure 2** The spatial distribution of dominant tree species by total biomass and species recruitment by largest number of new cohorts within each 12 km grid cell simulated under baseline climate and wildfire (BSWF) and projected climate and wildfire (CCWF). (a) Pixel values mapped at each grid cell are species with the highest biomass across five replicate runs and three climate models by late-century (2100). (b) The hybrid bar plot shows the percentage of the landscape occupied by the species classes mapped in panel a within each elevation band under BSWF and CCWF. Mean and standard error of aboveground C by elevation band are presented using the right y-axis. Values are based on the mean across five replicate runs of the three climate models. (c) Pixel values mapped at each grid cell are the species with the largest number of new cohorts over the course of simulation across five replicate runs and three climate models. (d) The bar plot shows the percentage of the landscape occupied by the species classes mapped in panel c within each elevation band under BSWF and CCWF.

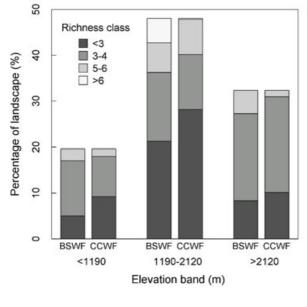
**Figure 3** The proportion of the landscape occupied by tree species richness class by elevation band under baseline climate and wildfire (BSWF) and projected climate and wildfire (CCWF). Values are based on the most frequent richness class within the 12 km grid cells across three climate models and five replicate runs by late-century (2100). **Figure 4** Mean and standard error of landscape Net Ecosystem C Balance (NECB) in each elevation band for baseline climate and wildfire and projected climate and wildfire under each climate model over the simulation period. Projected values are from five replicate simulations for each climate model. Baseline values are from three climate models and five replicate simulations.

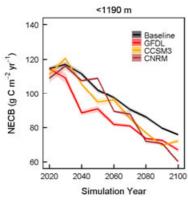
**Figure 5** Percentage of land area in each elevation band that is a C source by late-century for each climate model under baseline climate and wildfire (BSWF) and projected climate and wildfire (CCWF). Values are mean and standard error for five replicate simulations for each climate model.

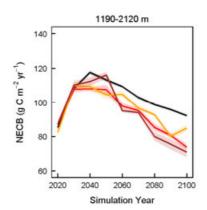


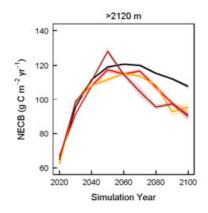


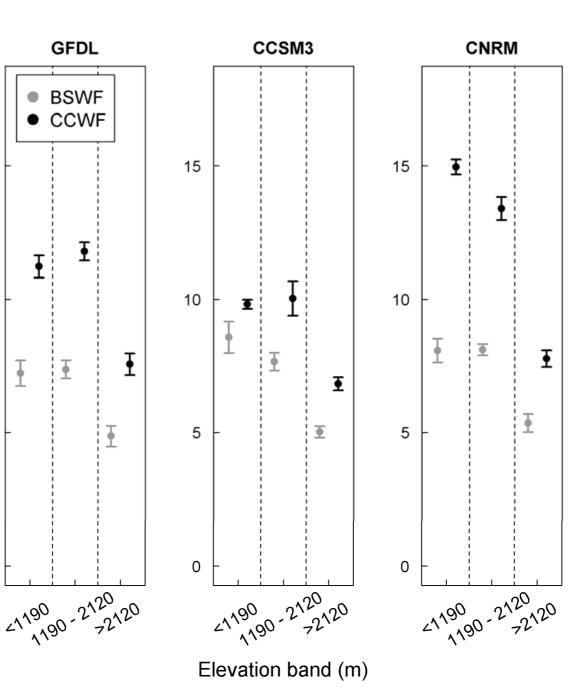
Elevation band (m)











**GFDL** 

**BSWF CCWF** 

Ŧ

Ŧ

Ŧ

Ī

Ī

15

10

5

0